

# Electron Transport in the Nanostructured TiO<sub>2</sub>–Electrolyte System Studied with Time-Resolved Photocurrents

Anita Solbrand, Henrik Lindström, Håkan Rensmo, Anders Hagfeldt,\* and Sten-Eric Lindquist\*

Department of Physical Chemistry, Uppsala University, P.O. Box 532, S-751 21 Uppsala, Sweden

Sven Södergren

Department of Physics, Uppsala University, P.O. Box 530, S-751 21 Uppsala, Sweden

Received: September 12, 1996; In Final Form: January 15, 1997<sup>®</sup>

Laser flash induced photocurrent transient measurements have been used to investigate the electron transport in nanostructured TiO<sub>2</sub> (anatase) thin film electrodes in contact with an electrolyte. The shape and the time domain for the current transients were found to be dependent on film thickness and electrolyte conductivity. The experimental results are discussed using a diffusion model. If the experimental results are interpreted as diffusion, a chemical diffusion coefficient for the electrons in the nanostructured system is determined to  $1.5 \times 10^{-5} \text{ cm}^2/\text{s}$  using 700 mM LiClO<sub>4</sub> in ethanol as electrolyte.

## I. Introduction

Considerable attention has recently been directed towards nanostructured semiconductor thin films in contact with an electrolyte.<sup>1</sup> These films exhibit a large potential in various fields of applications like solar energy,<sup>2,3</sup> batteries, displays,<sup>4</sup> and catalysis.<sup>5</sup> Understanding the charge transport is of importance for these systems. Since the nanostructured materials contain a significant amount of grain boundaries and have a high internal surface area in contact with the electrolyte, one might expect the electron transport properties to differ from a compact bulk semiconductor. Several mechanisms for the electron transport have been suggested, e.g., a hopping type of mechanism<sup>6,7</sup> and the possibility of tunneling through a potential barrier between the particles.<sup>8,9</sup> In a system with no macroscopic electric field both processes may be considered as a random motion between equivalent sites, i.e., diffusion. A diffusion model for the electron transport under steady state illumination has been derived describing the experimental observations of nanostructured electrodes in contact with electrolytes.<sup>14</sup> Time-resolved measurements of the potential dependence of the electron transport have been made for nanostructured ZnO,<sup>9</sup> TiO<sub>2</sub>,<sup>10,11</sup> and dye-sensitized TiO<sub>2</sub>.<sup>12,13</sup> The dependence of the film thickness and the electrolyte has only briefly been mentioned in these works. In the present work, photocurrent transients were recorded for nanostructured TiO<sub>2</sub> as a function of film thickness, electrolyte conductivity, and composition. The data are discussed by using the time-dependent diffusion equation, and a relation is derived to determine the diffusion coefficient. The mechanism of the diffusion process is not discussed and is left open for further studies.

## II. Theoretical Approach

The system considered in the present study consists of a nanocrystalline porous semiconductor (metal oxide) film electrode. The supporting electrolyte penetrates the film all the way to the back-contact. The oxide is assumed to be low doped or even undoped; i.e., the concentration of free charge carriers is low.

Consider the nanostructured system perturbed by a short laser pulse with a photon energy exceeding the band gap. The absorption profile of the light pulse generates the initial distribution of excited charge carriers in the nanostructured film. The thickness of the film and the wavelength of the light can be chosen in such a way that the intensity profile of the incident light has a sharp decay compared to the thickness of the film. Hence, if we illuminate directly on the film, the major part of the light will be absorbed in a very thin layer in the outer region of the electrode far from the back-contact.

The relaxation of the excited nanocrystalline system following the light absorption can qualitatively be described as follows: Immediately after the laser pulse, before any charge transfer into the electrolyte or any transport of charges between interconnected crystallites occurs, a fraction of the photogenerated carriers will recombine in the bulk of the crystallites. Due to differences in the overall kinetics for electron and hole transfer into the solution, either of the remaining free carriers is preferentially transferred into the electrolyte. This causes a charge separation of the electrons and holes. If, for instance, the holes quickly reaches the surface of the crystallites and oxidize a species in the solution, the excited electrons left behind will be stored in the conduction band of the crystallites. The inhomogeneously induced concentration of excited electrons implies a gradient in electrochemical potential in the film. This driving force causes the electrons to move in the direction toward the back-contact (toward lower electrochemical potential). In this case the driving force is the sum of the electrostatic repulsion and the concentration gradient of the excited electrons in the crystallites.

Depending on the concentration of excited electrons inside the crystallites (i.e., light intensity), the magnitude of the electrostatic repulsion will be different. The electrostatic repulsion will force some of the electrons towards the back-contact. The reorganization of the electrolyte that follows gives rise to a current  $I_{RC}$  at the back-contact which may be approximated by an RC circuit.

\* Authors to whom correspondence should be addressed.

<sup>®</sup> Abstract published in *Advance ACS Abstracts*, March 15, 1997.

$$I_{RC} \approx (q'/\tau)e^{-t/\tau} \quad (2.1)$$

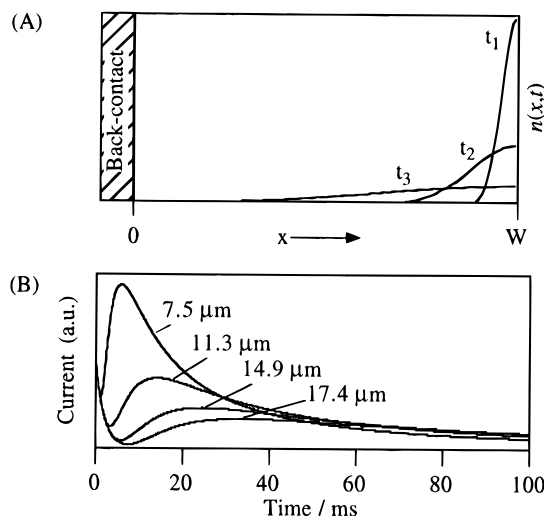


**Figure 1.** (A) Schematic picture of the TiO<sub>2</sub> thin film electrode after excitation by a laser pulse in the outermost layer. The evolution of the electron concentration is shown at three different times,  $t_1 < t_2 < t_3$ . (B) Simulated transients, eq 2.5, with  $\tau = 2$  ms,  $D = 1.5 \times 10^{-5}$  cm<sup>2</sup>/s, and  $W$  as indicated in the figure.

$q'$  is the charge affected at the back-contact, and  $\tau$  is the time constant for the RC circuit.

After the reorganization of the electronic repulsion, we assume that the electrostatic forces between excited electrons within the crystallites can be neglected. To obey the overall condition of charge neutrality, the movement of a photoexcited electron *between* the interconnected particles must be counterbalanced by a reorganization of the oppositely charged ion clouds in the surrounding electrolyte, an *image charge*. The conductivity of the electrolyte phase measures the ability to transport charges through this phase. Hence, it can be expected that the transport properties of electrons within the film are dependent on the conductivity of the electrolyte in the cavities of the film. By increasing the conductivity of the electrolyte, the excited electrons traversing through the network of particles are more easily charge compensated, and the transit time for the photogenerated electrons through the film will therefore in general decrease.

The electron and the image charge will move because of thermal fluctuations in the system. This results in a random walk process, diffusion, for the motion of the interacting charges. With increasing thickness of the nanostructured film the carriers will on average have a longer distance to travel. Hence, the transit time will be longer for thicker films. During the transport to the back-contact the electrons can be lost to electron-accepting species in the electrolyte, e.g., species previously oxidized by the hole, or other redox active species.

To derive the diffusion current, we will solve the time-dependent diffusion equation (Fick's second law) for electrons with a known initial distribution

$$\frac{\partial n(x,t)}{\partial t} = D \frac{\partial^2 n(x,t)}{\partial x^2} \quad (2.2)$$

$D$  is the chemical diffusion coefficient for the electron coupled to its image charge,  $x$  is distance from the back-contact,  $t$  is time, and  $n$  is electron concentration. The derivation is made for illumination directly on the film; see Figure 1A. In the derivation, the initial distribution is approximated with a square pulse of negligible width containing  $\Delta N$  photoexcited electrons after initial recombination and reorganization. We neglect recombination during the diffusion process. The solution with

the square pulse located at the outermost layer of the electrode  $x = W$  is

$$n(x,t) = \frac{\Delta N}{2\sqrt{\pi Dt}} e^{-(x-W)^2/4Dt} \quad (2.3)$$

The current equals the electron concentration gradient times the diffusion coefficient for the electrons and the elementary charge  $q$ . When deriving the expression for the current, we take into account that the electrons are reflected at the boundary  $x = W$ . The diffusion current  $I_{\text{diff}}$  at the back-contact  $x = 0$  is

$$I_{\text{diff}} = \frac{qW\Delta N}{2\sqrt{\pi Dt}^{3/2}} e^{-W^2/4Dt} \quad (2.4)$$

The total transient is the sum of the diffusion current (eq 2.4) and the current originating from the electrostatic repulsion (eq 2.1)

$$I = \frac{qW\Delta N}{2\sqrt{\pi Dt}^{3/2}} e^{-W^2/4Dt} + \frac{q'}{\tau} e^{-t/\tau} \quad (2.5)$$

In Figure 1B theoretical current transients are plotted. For thick films two components (peaks) are present. The fast component is from  $I_{RC}$ , and the slow originates from diffusion. With increasing film thickness we notice three major features: a delay and a decrease of the current maximum (for  $t > 0$ , i.e., the diffusion process) and a broadening in the current transient due to slower decay.

If  $I_{RC}$  is fast or small compared to the diffusion, the transient has a characteristic maximum. The current is at maximum when

$$dI/dt = 0 \quad (2.6)$$

Neglecting  $I_{RC}$ , the time for the current maximum  $t_{\text{peak}}$  appears when

$$t_{\text{peak}} = W^2/6D \quad (2.7)$$

Thus, in case of diffusion we expect a linear dependence between the square of the film thickness and the time for the current maximum with a slope of  $6D$ .

The neglect of the Coulomb interaction *in* and *between* the nanocrystallites may be motivated as follows. The Coulomb interaction between nanocrystallites will be small due to the screening of the electrolyte. The effects from electron–electron interactions within a single nanocrystallite are partially taken into account with  $I_{RC}$ . The interactions between photoexcited electrons will increase at higher light intensities and immediately after the absorption process because of the high local electron concentration. At longer times the electron interactions will decrease since the distance between the moving electrons increases. In the case of TiO<sub>2</sub> the high dielectric constant of the material also favors the neglect of electron–electron interaction.

### III. Experimental Section

**A. Electrode Preparation and Characterization.** The TiO<sub>2</sub> colloidal suspension was prepared by hydrolysis of titanium isopropoxide as described in ref 3; the autoclaving temperature was 200 °C. This procedure gives a colloid radius of about 7 nm. The electrodes were prepared by applying the colloidal suspension on a conducting glass substrate (Libbey Owens Ford (LOF), fluorine-doped SnO<sub>2</sub> glass, sheet resistance 8 Ω/□) with a Scotch tape as frame and spacer and raking off the excess

solution with a glass rod. Film thickness between 4 and 17  $\mu\text{m}$  were obtained by repeating the procedure 1–4 times. The electrodes were sintered in 450  $^{\circ}\text{C}$  in air for 30 min after each application. The film thicknesses were measured with an accuracy of 5%, using a Tencor Alpha Step profilometer. The porosity of the films was determined to 60% (the volume percent of  $\text{TiO}_2$ ), using the film area, thickness, weight, and the bulk density of anatase  $\text{TiO}_2$ . The films consist of pure anatase as determined by X-ray diffraction.<sup>16</sup>

**B. Electrolyte.** The electrolytes were prepared from HPLC grade acetonitrile (Merck), milli-Q water, and 99.6% ethanol, spectroscopic quality (Kemetyl). The solutes used,  $\text{LiClO}_4$ , KSCN, and KI, were reagent grade. To adjust the pH of the water solutions, HCl was used. The conductivity of the solutions were measured at 25  $^{\circ}\text{C}$  using a HI 8333 conductivity meter, calibrated with 0.100 M KCl in water. The absorbance of all electrolytes and the cell at 308 nm was less than 0.05, which assures negligible absorption of the laser pulse.

**C. Cell and Apparatus.** The measurements were performed in a conventional three-electrode cell consisting of a quartz cuvette. The working electrode was the nanostructured  $\text{TiO}_2$  thin film electrode, and the counter electrode was a platinum foil. The applied potential was 300 mV vs Ag/AgCl in ethanol during all measurements. At this potential the photocurrent reaches a plateau, while the dark current is low.<sup>17</sup> Shifting the potential 50 mV in either direction did not change the current transient significantly. The potentiostat used was an EG & G Princeton Applied Research, Model 273. The rise time of the potentiostat was measured by applying a square wave potential, measuring the time for the outgoing signal to reach from 10 to 90% of the maximum value. The rise time never exceeded 10  $\mu\text{s}$ . The time for the potentiostat to resume the constant potential after the laser flash was less than 1  $\mu\text{s}$ . The current transients were monitored by a digital oscilloscope (Hewlett-Packard 54600A, 100 MHz, 1 M $\Omega$ ). The light source was a single-shot excimer laser (ELI-94, Estonian Academy of Sciences) with a pulse duration of 30 ns and wavelength of 308 nm. The energy per pulse was approximately 200 mJ, varying about 5% between pulses recorded the same day. The laser pulse was defocused, and the electrodes were illuminated homogeneously directly on the  $\text{TiO}_2$  (Figure 1a). The geometric areas of the electrodes were between 0.3 and 0.5  $\text{cm}^2$ , and approximately one-third of the laser pulse hit the electrode. Each transient reported is an average of five measurements performed with at least 3 min intervals in between. All measurements reported were performed in air. The amplitude of the current transients changed less than 10% when measured in argon or oxygen atmosphere compared to measurements in air.

#### IV. Results and Discussion

The charge separation in colloidal  $\text{TiO}_2$  after laser excitation is in the subnanosecond range.<sup>15</sup> The electrode is illuminated from the  $\text{TiO}_2$ –electrolyte interface side, and the electron concentration profile after the charge separation should have a similar shape as the absorption profile. The upper limit of the penetration depth of the light is given by the exponential absorption profile due to the Lambert–Beer law. The absorption coefficient of  $\text{TiO}_2$  at 308 nm is in the  $10^{-7} \text{ m}^{-1}$  range,<sup>18</sup> which gives a penetration depth of the light of 0.2  $\mu\text{m}$ ; i.e., after 0.2  $\mu\text{m}$  99% of the light is absorbed. The electrode is probably light scattering at 308 nm. Thus, the penetration depth of the light will be even shorter and hence narrow the excited electron distribution. This makes the approximation of the initial distribution as a square pulse of negligible width valid. The thinnest film used was 4.1  $\mu\text{m}$ .

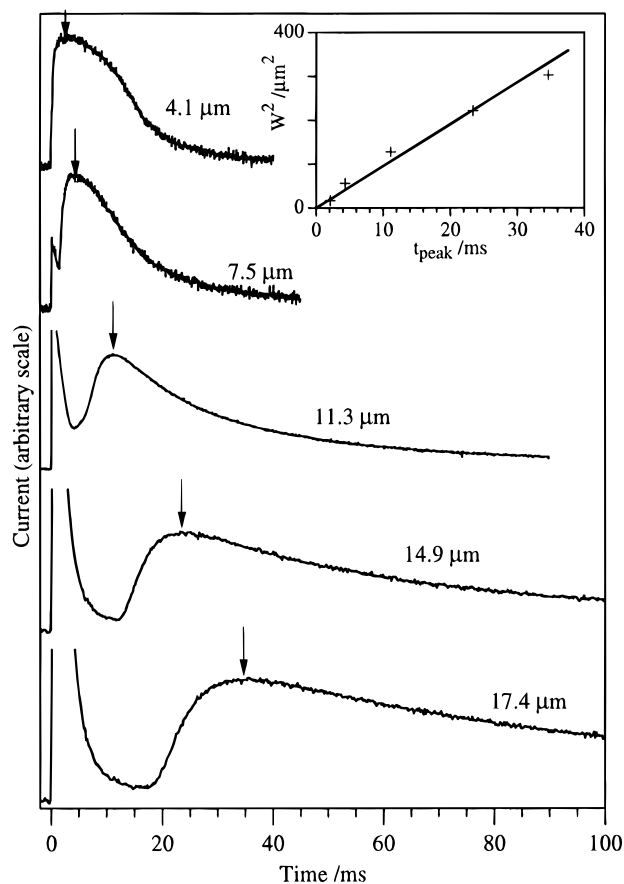


**Figure 2.** Photocurrent in arbitrary units vs time for electrodes of five different film thicknesses measured in 700 mM  $\text{LiClO}_4$  in ethanol. The film thicknesses are given in the graph. The characteristic current peak is marked with an arrow on each transient. The inset shows the time for the current peak vs the square of the film thickness. From the slope of the line the diffusion coefficient of the electrons  $D$  is determined to be  $1.5 \times 10^{-5} \text{ cm}^2/\text{s}$ .

**A. Dependence of Film Thickness.** The photocurrent transients for different film thickness are shown in Figure 2. The electrolyte was 700 mM  $\text{LiClO}_4$  in ethanol. Two current maxima are clearly visible in all transients, except for the thinnest electrode where they overlap. A similar shape of the transient have been observed earlier.<sup>10,11</sup> The transients are discussed in terms of a slow and a fast component. The amplitude of the first current peak, the fast component, is of the same range in all transients, and the rise time is in the range of the potentiostat. Moreover, the charge collected in the fast component of the transient is less than 5% of the total charge. The fast component in Figure 2 may be interpreted as a reorganization of charges after the laser pulse excitation, as discussed in section II. Unfortunately, the data of the fast component does not allow for a more detailed analysis.

The position of the maximum of the slow part of the transient is shifted to longer times with increasing film thickness, i.e., the longer distance the electrons have to travel. The decay of the current transients is slower with increasing film thickness. The maximum amplitude of the slow part of the transient also decreases with increasing film thickness. The experimental observations are in qualitative agreement of what is expected from a diffusive process. Therefore, the slow component of the transient can at least qualitatively be interpreted as photo-excited electrons diffusing to the back-contact. A straight line is obtained if we plot the peak time  $t_{\text{peak}}$  vs  $W^2$ , the inset in Figure 2. The straight line in this plot also permits a diffusion interpretation.

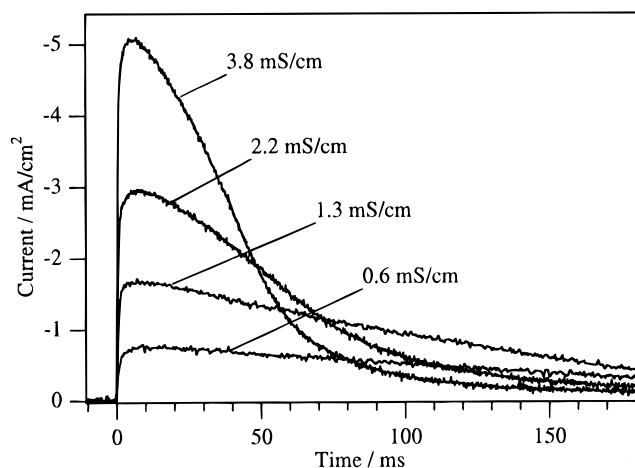


**Figure 3.** Photocurrent vs time for a 4.1  $\mu\text{m}$  thick electrode measured in  $\text{LiClO}_4$  in ethanol with four different conductivities. The conductivities of the solutions are shown in the graph. The concentrations of the electrolytes are 20, 50, 100, and 200 mM.

If the experimental results are interpreted as macroscopic electron diffusion through the film, a chemical diffusion constant of  $1.5 \times 10^{-5} \text{ cm}^2/\text{s}$  is determined for the electrons, using eq 2.7. The value is strikingly similar to the diffusion constant of ions in solutions. In contrast, the diffusion constant of electrons in compact  $\text{TiO}_2$  (rutile) has been determined to  $0.02 \text{ cm}^2/\text{s}$  and to  $0.01 \text{ cm}^2/\text{s}$  inside nanocrystallites of anatase  $\text{TiO}_2$ ,<sup>12,19</sup> which is several orders of magnitude higher compared to our result. This indicates that the electron transport is affected by the nanoporous structure of the film, e.g., the contact with the electrolyte throughout the film, and not only by interaction with the crystal lattice.

The total amount of collected charge decrease with increasing film thickness, showing higher losses due to the longer transport distances in thicker films. The difference in the total amount of charge between the thickest and the thinnest film, 17.4 and 4.1  $\mu\text{m}$ , respectively, is less than a factor of 3.

The simulated transients (eq 2.5) with experimental values of  $W$  and  $D$  are shown Figure 1B. The current is in arbitrary units since the exact light intensity is unknown. The time constant of the  $RC$  circuit is set to 2 ms, which is a reasonable value ( $\tau = RC$ ,  $C$  is 20–200  $\mu\text{F}$  and  $R$  is 10–100  $\Omega$ ). The agreement with the experimental results is satisfactory, considering that the model does not take into account for example recombination (except initial) or trap filling.

**B. Electrolyte Conductivity.** In Figure 3, the current transients for different conductivities of the electrolyte consisting of  $\text{LiClO}_4$  in ethanol are reported for a 4.1  $\mu\text{m}$  thick film. The amplitude decreases and the current decays slower with decreasing electrolyte conductivity. This shows a clear interaction between the electrons in the  $\text{TiO}_2$  and the ions in the electrolyte, as suggested in ref 9. The significant slowdown in decay of the transient and the magnitude of the diffusion coefficient (cf. Figure 2) indicates that the interaction between the electrons and the charge-compensating ion cloud in the electrolyte, the image charge, plays a dominant role in the charge transport mechanism of nanostructured materials in contact with an electrolyte. The photocurrent transients for nanostructured  $\text{ZnO}$  reported by Hoyer and Weller<sup>9</sup> are strikingly similar (in both shape and time aspect) to the transient reported here. Thus, it might be the case that the electron transport properties in nanostructured system depend more on the electrolyte and less on the type of material used to build the film. This is in contrast to compact crystals where the electron transport properties only depend on the interaction with the crystal lattice, unless the

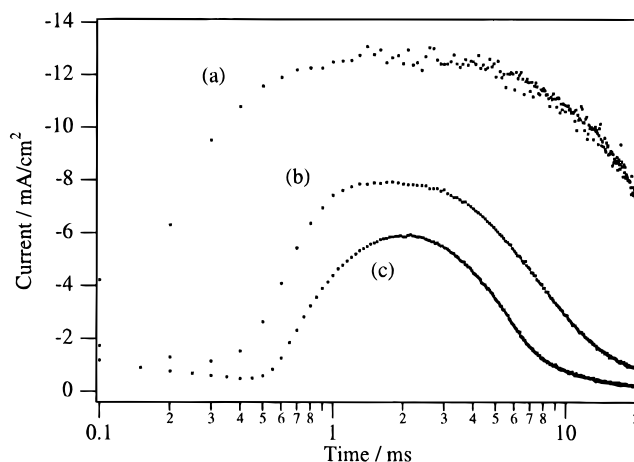


**Figure 4.** Photocurrent vs time for a 4.1  $\mu\text{m}$  thick electrode measured in three different electrolytes with equal conductivity, 9.3 mS/cm. The compositions of the electrolytes were (a) 740 mM  $\text{LiClO}_4$  in ethanol, (b) 100 mM KSCN in acetonitrile, and (c) 59 mM KI in water, pH = 2.52.

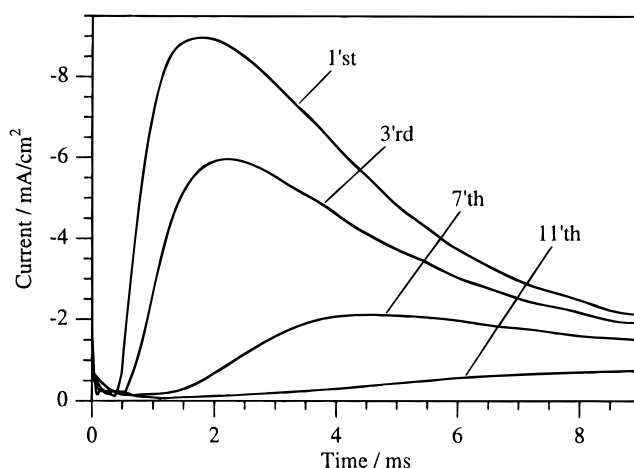


**Figure 5.** Photocurrent vs time for a 4.1  $\mu\text{m}$  thick electrode measured in 500 mM  $\text{LiClO}_4$  in acetonitrile. The electrode has been exposed to consecutive laser pulses with about half a second intervals of which the first, third, seventh and eleventh were recorded.

electron is located at the surface, making the interaction with the electrolyte feasible.

**C. Electrolyte Composition.** Figure 4 shows a logarithmic plot of the current transients for three different electrolyte compositions,  $\text{LiClO}_4$  in ethanol, KSCN in acetonitrile, and KI in water, pH = 2.52, with the same conductivity, 9.3 mS/cm. The film thickness was 4.1  $\mu\text{m}$ . The amplitude of the current changes with the electrolyte, while the shape of the transient and the time for the current maximum is similar. The similar profiles for the current maximum indicate that the movement of the electrons depends mainly upon the electrolyte conductivity and not on the composition. The change in the amplitude and decay in Figure 4 is interpreted as different recombination kinetics for the different electrolyte compositions. For instance, an effective hole scavenger, like ethanol, will quickly remove the valence band hole, leading to a lower initial electron–hole pair recombination inside the crystallites, which results in a higher photocurrent.

**D. Consecutive Pulses.** A deteriorating effect is observed when the measurements are performed with time intervals of about half a second. In Figure 5 the current transients of a 4.1  $\mu\text{m}$  thick electrode are displayed where each measurement has a different number of preceding laser light exposures with about half a second intervals. The electrolyte is 500 mM  $\text{LiClO}_4$  in

acetonitrile. The amplitude decreases and the current maximum of the slow component of the transient is delayed with increasing number of laser light exposures. The current transient resumes the same shape and magnitude after the electrode has rested a few minutes in the dark. The deterioration seen in Figure 5 is probably due to a progressive change in the electrolyte composition at the semiconductor–electrolyte interface. Similar observations have been made for steady state illumination.<sup>17</sup>

One could assume that trap filling might be a dominant part of the charge transport. If the electrons remain in traps for seconds, we would expect a faster rise time and a higher amplitude of the slow component of the transient when several laser pulses are applied consecutively, because fewer traps would be available. Instead, the opposite is observed after consecutive laser pulses. The deep trap filling process can be a small and constant effect, but it cannot be distinguished from losses in this measurement.

## V. Conclusions

The electron transport in nanostructured TiO<sub>2</sub> has been studied by time-resolved photocurrent measurements. The main features of the current transients after laser excitation can be discussed in terms of electron diffusion and recombination. A diffusion process to describe the electron transport in nanostructured systems has earlier been proposed for steady state illumination.<sup>14</sup> If the experimental results are interpreted as diffusion, a chemical diffusion coefficient for electrons in the nanostructured electrode in 700 mM LiClO<sub>4</sub> in ethanol is determined to  $1.5 \times 10^{-5}$  cm<sup>2</sup>/s. This is in the range of the diffusion constant for ions in the electrolyte and several orders of magnitude smaller than the diffusion constant for electrons in bulk TiO<sub>2</sub> (rutile)<sup>12</sup> or *inside* anatase colloids.<sup>19</sup> We also see a clear influence on the charge transport with different electrolyte conductivities. This indicates that the interaction between the electrons and the charge-compensating ion cloud in the electrolyte plays a dominant role in the charge transport in nanostructured materials in contact with an electrolyte. A reversible deteriorating effect

is observed when the measurements are performed with about half a second intervals and is probably due to a buildup of electron scavenging species in the pores of the electrode.

**Acknowledgment.** This work has been supported by the Swedish Research Council for Engineering Sciences (TFR), the Swedish Natural Science Research Council (NFR), and the commission of the European Community Joule II program. We thank Dr Jan Alsins for helping us with the laser.

## References and Notes

- (1) Hagfeldt, A.; Grätzel, M. *Chem. Rev.* **1995**, *95*, 49–68.
- (2) O'Regan, B.; Grätzel, M. *Nature* **1991**, *353*, 737–40.
- (3) Nazeeruddin, M. K.; Kay, A.; Rodicio, I.; Humphrey-Baker, R.; Müller, E.; Liska, P.; Vlachopoulos, N.; Grätzel, M. *J. Am. Chem. Soc.* **1993**, *115*, 6382–90.
- (4) Hagfeldt, A.; Vlachopoulos, N.; Grätzel, M. *J. Electrochem. Soc.* **1994**, *141*, 82–84.
- (5) Vinodgopal, K.; Hotchandani, S.; Kamat, P. V. *J. Phys. Chem.* **1993**, *97*, 9040–44.
- (6) Könenkamp, R.; Henniger, R.; Hoyer, P. *J. Phys. Chem.* **1993**, *97*, 7328.
- (7) Kay, A.; Humphrey-Baker, R.; Grätzel, J. *J. Phys. Chem.* **1994**, *98*, 952.
- (8) Hoyer, P.; Eichberger, R.; Weller, H. *Ber. Bunsen-Ges Phys. Chem.* **1993**, *97*, 630.
- (9) Hoyer, P.; Weller, H. *J. Phys. Chem.* **1995**, *99*, 14096–100.
- (10) Björkstén, U. On the Photo-Electrochemistry of Nanocrystalline Porous Semiconducting Metaloxide Electrodes. Thesis Nrl345, EPFL, Lausanne, Switzerland, 1995.
- (11) Hagfeldt, A. *Sol. Energy Mater.* **1995**, *38*, 339–41.
- (12) O'Regan, B.; Moser, J.; Anderson, M.; Grätzel, M. *J. Phys. Chem.* **1990**, *94*, 8720–26.
- (13) Schwarzburg, K.; Willig, F. *Appl. Phys. Lett.* **1991**, *58*, 2520–22.
- (14) Södergren, S.; Hagfeldt, A.; Olsson, J.; Lindquist, S.-E. *J. Phys. Chem.* **1994**, *98*, 5552–56.
- (15) Grätzel, M.; Frank, A. J. *J. Phys. Chem.* **1982**, *86*, 2964–67.
- (16) Lindström, H.; Rensmo, H.; Södergren, S.; Solbrand, A.; Lindquist, S.-E. *J. Phys. Chem.* **1996**, *100*, 3084–88.
- (17) Hagfeldt, A.; Lindström, H.; Södergren, S.; Lindquist, S.-E. *J. Electroanal. Chem.* **1995**, *381*, 39–46.
- (18) Lindquist, S.-E.; Finnström, B.; Tegnér, L. *J. Electrochem. Soc.* **1983**, *130*, 351–58.
- (19) Enright, B.; Fitzmaurice, D. *J. Phys. Chem.* **1996**, *100*, 1027–35.